Giant Amplification of Interfacially Driven Transport by Hydrodynamic Slip: Diffusio-Osmosis and Beyond

Armand Ajdari[1,2,3] and Lydéric Bocquet[4]

[1]*Physico-Chimie Théorique, UMR 7083 CNRS-ESPCI, 10 rue Vauquelin, 75231 Paris, France*
[2]*Department of Mathematics, MIT, Cambridge, Massachusetts 02139, USA*
[3]*DEAS, Harvard University, 29 Oxford Street, Cambridge, Massachusetts 02138, USA*
[4]*LPMCN, Université Lyon 1, UMR 5586 CNRS, 69622 Villeurbanne, France*

(Received 23 January 2006; published 10 May 2006)

We demonstrate that ''moderate'' departures from the no-slip hydrodynamic boundary condition (hydrodynamic slip lengths in the nanometer range) can result in a very large enhancement—up to 2 orders of magnitude—of most interfacially driven transport phenomena. We study analytically and numerically the case of neutral solute diffusio-osmosis in a slab geometry to account for nontrivial couplings between interfacial structure and hydrodynamic slip. Possible outcomes are fast transport of particles in externally applied or self-generated gradient, and flow enhancement in nano- or microfluidic geometries.

DOI: 10.1103/PhysRevLett.96.186102 PACS numbers: 68.08.−p, 47.61.−k, 47.63.Gd, 68.15.+e

Introduction.—The advent of ''microfluidics'' and ''nanofluidics'' has motivated the current great interest in understanding, modeling, and generating motion of liquids in artificial or natural networks of ever more tiny channels or pores [1]. Because of the huge increase in hydrodynamic resistance that comes with downsizing, two avenues for moving efficiently fluid at such scales have been revisited. Both rely on phenomena originating at the solid-liquid interface to take advantage of the increase of surface to volume ratio.

The first one is the *generation* of flow within the interfacial structure by application of a macroscopic gradient. Electro-osmosis, i.e., flow generation by an electric field, is the best known example which is commonly used in microfluidics [2]. But other surface-driven phenomena fall in the same category, such as diffusio-osmosis and thermo-osmosis where gradients of solute concentration and of temperature are used to induce solvent flow [3,4]. Their phenomenology is usually best described by an ''effective slip'' velocity, which quantifies the motion of the fluid with respect to the solid due to shearing forces in the usually thin interfacial layer [4].

The second is the amplification of pressure-driven flow by surfaces such that the fluid hydrodynamically ''slips'' on the solid, as usually quantified by the so-called slip length b [5] (the distance *within* the solid at which the flow profile extrapolates to zero). Recent efforts in this domain have concluded that with a clean ''solvophobic'' surface chemistry one can reach slip lengths up to a few ten nanometers [6], but not much more unless topographic structures are specifically engineered [7].

In this Letter, generalizing a point recently made for electro-osmosis [2,8,9], we argue that these two strategies can actually be synergetically combined, yielding strongly enhanced interfacial driven flows on solvophobic surfaces. More quantitatively, we argue that an actual ''hydrodynamic slip'' increases the ''effective slip velocity,'' which controls all manifestations of the interfacially driven phenomena, by a factor $(1 + b/L)$, where b is the hydrodynamic slip length and L a measure of the interfacial thickness. This ratio can be *of order ten to hundreds* in realistic situations, so that the enhancement described here can be very large. This synergy may lead to more efficient transduction of electrical, chemical, or thermal energy into mechanical work in microdevices.

Beyond the nano- or microfluidic interest in moving fluids in tiny solid structures, our considerations also apply to the reciprocal interfacially driven motion of solid particles in solution. We thus predict enhancement of electrophoresis, diffusiophoresis, and thermophoresis (induced, respectively, by gradients in electric potential, concentration of solutes, and gradients of temperature) when solvophobic particles are dispersed in solution. Our analysis may also be of relevance to the ''swimming'' of artificial or natural organisms by self-generation of such gradients [4,10–12].

To exhibit the physics at work, we first focus on diffusio-osmosis with a single neutral solute species, in the simplest geometry of a flat uniform interface. Using a continuum description for hydrodynamics with slip, we derive the $(1 + b/L)$ enhancement factor for that situation. A formal generalization to other interfacially driven phenomena is then presented. Further, a molecular dynamics study of diffusio-osmosis in a thin slab geometry quantitatively comforts the picture. We end with a brief discussion of the case of charged solutes (in particular electro-osmosis) and of the motion of finite-size particles.

Consider a flat homogeneous solid surface $y(x, z) = 0$, with an incompressible liquid of bulk viscosity η_0 in the $y > 0$ space. Slip is described through the Navier boundary condition (BC) for the velocity field $\boldsymbol{v}$, $b\partial_y v_i|_{y=0} = v_i|_{y=0}$ for $i = x, z$, with b the distance in the solid at which the linearly extrapolated velocity becomes zero (see Fig. 1). In a slightly more general approach the hydrodynamic

"weakness" of the interface shows up in a y-dependent viscosity $\eta(y)$, while requiring $v|_{y=0} = 0$. The Navier BC is recovered using the ansatz $\eta^{-1}(y) = \eta_0^{-1}[1 + b\delta(y)]$, sketching slip in terms of a very thin vacuum layer of very low viscosity "between" the liquid and the solid.

Diffusio-osmosis for a neutral solute.—Suppose that the solution contains a single neutral solute, at bulk concentration c_0, which interacts with the wall through a short-range potential $U(y)$. In the dilute limit, at equilibrium the distribution of the solute is $c_{\rm eq}(y) = c_0 \exp(-\frac{U(y)}{k_B T})$. If a concentration gradient dc_0/dx is applied along x over long distances (compared to the range of the potential), equilibration of concentration and pressure is fast along y (compared to the relaxation time of the gradient), so that $c \simeq c_0(x)\exp(-\frac{U(y)}{k_B T})$ and $-\partial_y p(x,y) + c(x,y) \times (-\partial_y U) = 0$. This leads to the "osmotic" equilibrium $p(x,y) - k_B T c(x,y) = p_0 - k_B T c_0(x)$ [13], with p_0 the constant bulk pressure. As a consequence, a pressure gradient along x sets in (only) within the thin interfacial layer, $\partial_x p = k_B T \partial_x (c - c_0)$, which generates shear there through the hydrodynamic balance: $-\partial_x p(x,y) + \partial_y(\eta \partial_y v_x) = 0$. The fluid velocity increases accordingly through the interfacial layer to reach a finite value v_s, the "effective slip velocity" of the liquid past the surface due to the applied gradient along x (Fig. 1 sketches the case of a solute attracted to the wall, $\Gamma > 0$). Integrating twice along y and using the Navier BC:

$$v_s = -(k_B T/\eta_0)\Gamma L(1 + b/L)\frac{dc_0}{dx}, \qquad (1)$$

where $\Gamma = \int_0^\infty dy[e^{-U(y)/k_B T} - 1]$ is a length measuring the excess of solute in the vicinity of the surface (U is positive and Γ negative for depletion), and $L = \Gamma^{-1}\int_0^\infty dy y[e^{-U(y)/k_B T} - 1]$ measures the range of interaction of the potential. Equation (1) is the classical formula of Anderson and Prieve [13], times the amplification factor $1 + b/L$: this quantifies how hydrodynamic slip allows to generate a larger "effective slip" v_s away from the surface (Fig. 1). Physically v_s results from the balance between viscous shear stress at the interface corrected for slip, $\eta_0 v_s/(L + b)$, and the (integrated) body force within the interface layer: $-\frac{d}{dx}(\Gamma k_B T c_0)$.

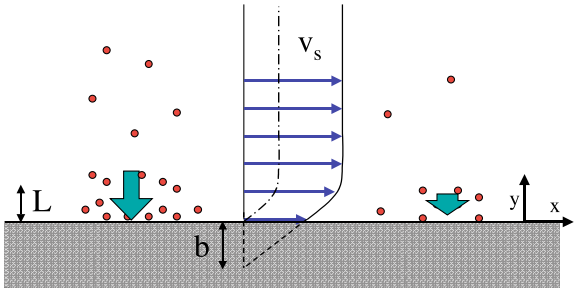

FIG. 1 (color online). Diffusio-osmosis for a neutral solute attracted to the solid (in gray). The larger bulk concentration on the left results in a higher accumulation of solute at the interface (thickness L) "squeezing" the fluid against the wall. A pressure gradient results *in* this L-thick interfacial layer, which induces shear there and a flow opposite to the concentration gradient. In contrast with the no-slip case ($b = 0$, flow depicted by the dot-dashed line), hydrodynamic slip (i.e., a nonzero extrapolation slip length b) allows these stresses to generate a larger "effective" diffusiophoretic slip v_s (to be distinguished from the very local slip velocity right at the wall).

The slip induced enhancement can actually be very large. For molecular interactions between neutral solutes and a solid L is very small, e.g., $\sim$0.3 nm, so with $b \sim$ 20–30 nm for water on hydrophobic substrates [5,6], the amplification factor can be up to 100.

Formal general argument.—We now generalize this result. For a generic interfacial structure, denote σ_n and σ_t the stresses normal and tangential to the interface which develop in a thin layer close to the solid [4]. At equilibrium, the situation is invariant by translation along x, so $\sigma_n = \sigma_n(y)$ and $\sigma_t = \sigma_t(y)$, and the hydrostatic pressure $p(y)$ is determined by force balance $-\partial_y p + \partial_y \sigma_n = 0$, $-\partial_x p + \partial_x \sigma_t = 0$, yielding $p(y) = p_0 + \sigma_n(y)$, with again p_0 the constant bulk pressure.

If a small far-field gradient of an observable O (concentration, potential, temperature) is applied along x then the interfacial stresses vary slowly along x, too. Pressure equilibration is fast in the y direction and $-\partial_y p + \partial_y \sigma_n = 0$ yields $p(x,y) = p_0 + \sigma_n(x,y)$. The resulting lateral imbalance of pressure, within the interfacial layer, generates shear along x as described by the force balance $-\partial_x p + \partial_x \sigma_t + \partial_y(\eta(y)\partial_y v_x) = 0$. Again, this generates an "effective slip" v_s which reads [using $\eta(y)$ and $v(y = 0) = 0$]

$$v_s = -\frac{d}{dx}\left[\int_0^\infty dy \Sigma(x,y)\int_0^y dy' \eta^{-1}(y')\right] \qquad (2)$$

with $\Sigma(x,y) = \sigma_n - \sigma_t$ the interfacial stress anisotropy. If the structure of the interface varies slowly along x, $\Sigma \simeq \Sigma_{\rm eq}[y, O(x)]$, where $O(x)$ is the "outer" value of the field O outside the interfacial layer, so that the effective slip generated by dO/dx is

$$v_s = -\frac{1}{\eta_0}\int_0^\infty dy \frac{\partial \Sigma_{\rm eq}}{\partial O}(y)\left[y + \int_0^y dy' \frac{\eta_0 - \eta(y')}{\eta(y')}\right]\frac{dO}{dx}. \qquad (3)$$

The integral in the bracket quantifies the specific contribution of the hydrodynamic slip. For a slip length b [using $\eta_0/\eta(y) = 1 + b\delta(y)$], we obtain our main result:

$$v_s = -\frac{1}{\eta_0}\Gamma L[1 + b/L]\frac{dO}{dx}, \qquad (4)$$

where $\Gamma = \int_0^\infty dy \frac{\partial \Sigma_{\rm eq}}{\partial O}(y)$, and $L = \Gamma^{-1}\int_0^\infty dy y \frac{\partial \Sigma_{\rm eq}}{\partial O}(y)$ is a measure of the thickness of the stress-generating interface that depends on the observable O considered. The case of (neutral solute) diffusio-osmosis is recovered with: $\sigma_n = k_B T(c - c_0)$, $\sigma_t = 0$, $O = k_B T c_0$, and $\frac{\partial \Sigma_{\rm eq}}{\partial O} = (c_{\rm eq} - c_0)/c_0 = e^{-U(y)/k_B T} - 1$.

The results obtained so far rely on a continuum description of the interface hydrodynamics. To demonstrate that the enhancement persists in a more realistic context, we turn to a slab geometry that we will analyze using numerical simulations.

Diffusio-osmosis in a channel.—Let us consider a channel of width H. In the linear response regime a symmetric matrix relates the fluxes (per unit length) in the x direction (Q, J) to the gradients $(-\nabla\pi, -\nabla\mu)$ that generate them, with Q the total flow rate, J the total solute current, $\pi = p - k_B T c$ the pressure corrected for osmotic effects, and $\mu \simeq \mu_0 + k_B T \ln(c)$ the chemical potential of the solute [14,15]. Equivalently, diffusio-osmosis is best described by the following matrix M quantifying net transport through the channel:

$$\begin{bmatrix} Q \\ J - c_0 Q \end{bmatrix} = \begin{bmatrix} M_{11} & M_{12} \\ M_{21} & M_{22} \end{bmatrix} \begin{bmatrix} -\nabla p \\ -k_B T \nabla c_0 / c_0 \end{bmatrix}. \quad (5)$$

Onsager reciprocity relations require $M_{12} = M_{21}$ [14,15], which we explicitly checked by solving the continuum hydrodynamic problem with a slip length b on the two walls in the two situations $\nabla p \neq 0$, $\nabla c_0 = 0$ and $\nabla p = 0$, $\nabla c_0 \neq 0$ [16]. In the latter situation and for channels wider than the interfacial structures ($H \gg L$), we obtain as expected a pluglike flow driven by a concentration gradient: $Q = M_{12}(-k_B T \nabla c_0 / c_0) = H v_s$ with v_s the slip velocity given in Eq. (1), and $M_{12} = \frac{H c_0}{\eta_0} \Gamma (L + b)$. For thinner (nano) channels, the overlap between the interfacial layers must be taken into account [16].

Numerical simulations.—We then conduct molecular dynamics simulations of a fluid system composed of solvent + solute particles, confined between two parallel solid walls composed of individual "solid" particles fixed on a fcc lattice [17]. Interactions between the three types of particles are of Lennard-Jones type, $U_{\alpha\beta}(r) = 4\epsilon[(\frac{\sigma}{r})^{12} - u_{\alpha\beta}(\frac{\sigma}{r})^6]$, with identical interaction energy ϵ and molecular diameters σ ($\alpha, \beta \in \{\text{solute, solvent, walls}\}$). Tuning the parameters $u_{\alpha,\beta}$ we can vary (i) the wettability of the solvent on the wall by tuning $u_{\text{solvent,wall}}$, and (ii) the relative attraction or depletion of the solute to that wall (by tuning $u_{\text{wall,solute}}$ for a fixed $u_{\text{wall,solvent}}$). Periodic boundary conditions are used along x and z (box size $l_x = l_z = 16\sigma$), and the interwall distance is $l_y = H = 20.8\sigma$. Temperature is kept constant by applying a Hoover thermostat to the z degrees of freedom (i.e., perpendicular to flow and confinement). Solvent density is $\rho_f \sigma^3 \sim 0.9$, and bulk solute concentration $c_0 \sigma^3 \sim 0.02$. Rather long runs ($\sim 5 \times 10^6$ time steps) are performed to obtain good statistics.

To determine the cross coefficient $M_{12} = M_{21}$, the most efficient route is to apply an external volume force, $f_0 = -\nabla p$, to the fluid in the x direction, so as to generate a pressure-driven flow. We then measure the solute *excess current*, $J - c_0 Q$, associated with the convective motion of the solute [18], and obtain $M_{21} = (J - c_0 Q)/(-\nabla p)$, according to Eq. (5) (we check linearity of the response to the external force). Eventually we extract the adsorption length Γ from the equilibrium solute density profile $c(y)$ as $\Gamma = \frac{1}{2} \int_{\text{slab}} dy [c(y)/c_0 - 1]$. To narrow our exploration, we focus on the ideal solution of solvent and solute molecules identical but for their interactions with the walls. We take $u_{\text{solvent,solvent}} = u_{\text{solute,solute}} = u_{\text{solvent,solute}} = 1.2$, and consider three solvent-wall situations $u_{\text{wall,solvent}} = 0.3, 0.5, 1.0$ (going from nonwetting to wetting) and solute-wall interactions $u_{\text{wall,solute}}$ in the range $[0.1, 1.1]$. In all cases, the hydrodynamic velocity profiles are parabolic, which allows us to extract the viscosity η and the slip length b [19]. In agreement with previous work [19] and experimental results, slip is significant for a nonwetting solvent ($b \sim 20$–40σ for $u_{\text{wall,solvent}} \sim 0.3$–$0.5$), and negligible for a wetting solvent ($b \leq \sigma$ for $u_{\text{wall,solvent}} = 1$).

Figure 2 displays the outcome of our simulations for the cross coefficient $M_{21} = M_{12}$, normalized by a value $M_{12}^{(0)} = \frac{c_0}{\eta} \sigma H \Gamma$, which corresponds to a reference situation with a no-slip BC and fixed $L = \sigma$. In line with our theoretical arguments, M_{12} is strongly enhanced—$M_{12}/M_{12}^{(0)}$ up to 40 here—for nonwetting solvents ($u_{\text{wall,solvent}} = 0.3, 0.5$, top data), i.e., systems with slip lengths of a few tens of molecular diameters (i.e., roughly ~5–10 nm). On the other hand, M_{12} is much smaller ($M_{12} \sim M_{12}^{(0)}$) for a wetting solvent ($u_{\text{wall,solvent}} = 1$, bottom data), associated with a no-slip BC.

More quantitatively our MD results compare successfully to the theoretical prediction rewritten as $M_{12}/M_{12}^{(0)} = (L + b)/\sigma \simeq b/\sigma$ (since $L \lesssim \sigma \ll b$), see Fig. 2, provided we use the slip length b extracted from the simulation for each case. In particular, the amplification decreases

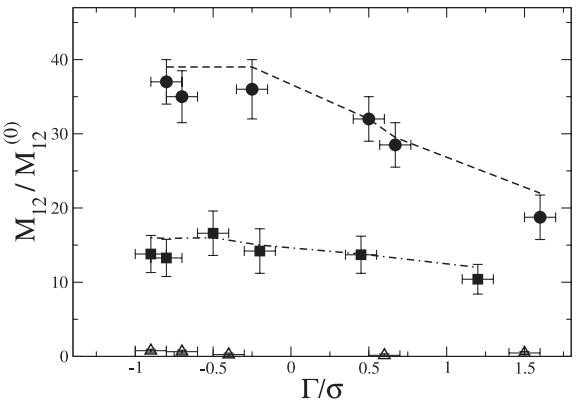

FIG. 2. Cross coefficient M_{12} for a slab geometry (normalized by a no-slip reference $M_{12}^{(0)} = \frac{c_0}{\eta} \sigma H \Gamma$), against normalized interfacial enrichment in solute Γ/σ, for wetting to nonwetting solvents $u_{\text{wall,solvent}} = 1.0$ (△), 0.5 (■), 0.3 (●), and $u_{\text{wall,solute}}$ in the range [0.1–1.1]. The dashed lines are the theoretical prediction $M_{12}/M_{12}^{(0)} = (L + b)/\sigma \simeq b/\sigma$ using the measured slip length b which is significant for the nonwetting cases: $b \sim 12$–16σ (■) and $b \sim 20$–40σ (●). For large positive adsorption, the enhancement decreases as does the slip length, because the adsorbed solute increases the fluid/solid wetting.

for large positive adsorptions $\Gamma > 0$, due to the decrease of the slip length: accumulation of "wetting" solute at the solid-liquid interface reduces the effective "solvophobicity" [20]. For a depleted solute, ($\Gamma < 0$), this "saturation" effect is essentially absent (b is nearly constant) allowing for large enhancements.

Electrolyte solutions: electro- and diffusio-osmosis.—For charged solutes, the interfacial structure is the electrical double layer, of typical thickness the Debye length κ^{-1} [3], usually in the nanometer range (1–30 nm), and we anticipate $L \sim \kappa^{-1}$. The enhancement of interfacially driven phenomena (electro-osmosis, diffusio-osmosis, thermophoresis) over solvophobic surfaces (b in the 20–30 nm range) should thus be somewhat smaller than for the neutral solute case, but still significant.

As a check of $L \sim \kappa^{-1}$, we incorporate a finite slip length b in the usual description of these phenomena [3], and compute the enhancement factor $(1 + b/L)$ in Eq. (4) [16]. For electro-osmosis $L = -\frac{\phi_{\rm eq}}{d\phi_{\rm eq}/dy}|_{y=0}$, with $\phi_{\rm eq}(y)$ the equilibrium electrostatic potential in the double layer, so for weakly charged surfaces $L \simeq \kappa^{-1}$ in agreement with [2,8,9]. For diffusio-osmosis and a 1:1 electrolyte, we obtain a more complex formula, with $L \simeq \kappa^{-1}/2$ for weakly charged surfaces.

Transport of particles.—All the above applies to the reciprocal motion of particles in concentration or potential fields, in a way that can be quite directly quantified provided the surface is locally flat and homogeneous at the L scale following [3,4,13]. Classically for interfacial driven effects, considering finite-size objects such as a spherical particle of radius $a \gg L$ allows one to discuss the possible feedback of the generated flow on the interfacial structure where it originates [13]. We compute here the diffusiophoresis of such a sphere generated by a steady background gradient of neutral solute, adapting the classical no-slip analysis of [13]. Including hydrodynamic slip (nonzero b) enhances the surface-liquid effective slip as described by (1), but also the convection of solute in the interfacial region, which affects the steady-state concentration field of the solute (diffusion coefficient D) around the particle. We find the velocity U of the particle in a solute gradient ∇c_0 to be

$$\mathbf{U} = \frac{k_B T}{\eta_0} L\Gamma \frac{1 + b/L}{1 + [1 + (\nu + b/L)Pe](\Gamma/a)} \nabla c_0 \qquad (6)$$

with $Pe = (k_B T/D\eta_0)L\Gamma c_0$ and ν a dimensionless quantity of order 1 defined in [13] that depends on the exact shape of the potential. For moderate values of $\Gamma \ll a$, the usual slip enhancement factor $(1 + b/L)$ prevails, and for $b \gg L$ the formula reads $U \simeq (k_B T/\eta_0) b\Gamma\nabla c_0$. For $\nabla c_0 \sim 10^{-3}$ mol/cm^4, $\Gamma \sim L \sim$ Å, and $b \sim 30$ nm, this leads to $U \gtrsim \mu$m/s (in contrast to $\sim$5 nm/s for the no-slip case), comparable to experimental observations of chemical self-propulsion [12]. For smaller particles or stronger solute adsorption ($\Gamma/a \gg 1$), the effect of slip saturates for large b/L (the large generated flow "erases" partly the original interfacial gradients), with a maximal velocity $U_{\rm max} = (k_B T/\eta_0)\frac{La}{Pe}\nabla c_0$ independent of b.

Conclusion.—Hydrodynamic slip can very significantly enhance many interfacially driven phenomena on smooth solvophobic surfaces. This is of relevance for the transport of fluids in small channels, and of particles in solutions. A related target is the modeling and engineering of the self-transport of chemically driven swimmers, for which the hydrophobicity of the surface is thought to play an important role [12]. Further study is necessary to go beyond the model smooth surfaces considered here, so as to assess the effect of topographic or chemical heterogeneities at various scales (e.g., roughness can potentially either increase or decrease slip effects in channels depending on whether or not it leads to gas entrapment).

[1] T. M. Squires and S. R. Quake, Rev. Mod. Phys. **77**, 977 (2005).
[2] H. Stone, A. Stroock, and A. Ajdari, Annu. Rev. Fluid Mech. **36**, 381 (2004).
[3] R. J. Hunter, *Foundations of Colloid Science* (Oxford University Press, New York, 1991).
[4] J. L. Anderson, Annu. Rev. Fluid Mech. **21**, 61 (1989).
[5] E. Lauga, M. Brenner, and H. Stone, *Handbook of Experimental Fluid Dynamics* (Springer, New York, 2006).
[6] C. Cottin-Bizonne, B. Cross, A. Steinberger, and E. Charlaix, Phys. Rev. Lett. **94**, 056102 (2005).
[7] J. Ou, B. Perot, and J. P. Rothstein, Phys. of Fluids **17**, 4735 (2004).
[8] L. Joly, C. Ybert, E. Trizac, and L. Bocquet, Phys. Rev. Lett. **93**, 257805 (2004).
[9] N. V. Churaev, J. Ralston, I. P. Sergeeva, and V. D. Sobolev, Adv. Colloid Interface Sci. **96**, 265 (2002).
[10] P. E. Lammert, R. Bruinsma, and J. Prost, J. Theor. Biol. **178**, 387 (1996).
[11] R. Golestanian, T. Liverpool, and A. Ajdari, Phys. Rev. Lett. **94**, 220801 (2005).
[12] W. F. Paxton, A. Sen, and T. E. Mallouk, Chem. Eur. J. **11**, 6462 (2005).
[13] J. L. Anderson and D. Prieve, Langmuir **7**, 403 (1991).
[14] S. R. De Groot and P. Mazur, *Non-Equilibrium Thermodynamics* (North-Holland, Amsterdam, 1969).
[15] E. Brunet and A. Ajdari, Phys. Rev. E **69**, 016306 (2004).
[16] A. Ajdari and L. Bocquet (to be published).
[17] We have used the MD code LAMMPS 2001, written by Steve Plimpton (Sandia Labs).
[18] c_0 is measured in the middle of the cell, where the solute density profile is flat; J and Q are measured, respectively, from the averaged solute current and solvent velocity profile.
[19] J.-L. Barrat and L. Bocquet, Phys. Rev. Lett. **82**, 4671 (1999).
[20] A simple empirical law quantitatively fits the numerical results for b: $1/b = (1 - x_0)/b_0 + x_0/b_1$, with $x_0 = c_0/\rho_f$ the solute volume fraction and b_0 (respectively b_1) the slip length for a pure solvent (respectively solute) system.